

Break-up of neutron-halo nuclei by diffraction dissociation and shakeoff

 F. Barranco¹, P.G. Hansen^{2,3}
¹ Escuela Superior de Ingenieros, Universidad de Sevilla, Av. de los Descubrimientos s/n, 41092 Sevilla, Spain

² National Superconducting Cyclotron Laboratory, Michigan State University, East Lansing, MI 48824, USA

³ Department of Physics and Astronomy, Michigan State University, East Lansing, MI 48824, USA

Received: 29 October 1999 / Revised version: 15 January 2000

Communicated by W. Weise

Abstract. The interplay of diffraction dissociation and nuclear shakeoff is considered in a schematic but still realistic model for the case of the break-up of halo nuclei on light targets. We demonstrate that the shakeoff effect, arising from the momentum imparted by the core diffraction, is small but still identifiable in the experimental data for the dissociation of the one- and two-neutron halo nuclei ^{11}Be and ^{11}Li .

PACS. 24.10.-i Nuclear-reactions models and methods

1 Introduction

Diffraction mechanisms are an important ingredient in the understanding of the break-up of neutron halo systems at intermediate and high energies [1-7]. The main effect arises from the diffraction of the halo neutron, which imparts a large momentum in the centre-of-mass (CM) system of the halo. In comparison to this, the momentum imparted by core diffraction is reduced by a factor $1/A$, where A is the core mass number, and break-up via this channel can to lowest order be neglected.

Core diffraction, on the other hand, is a dominating mechanism in the elastic scattering of halo nuclei on light targets. In an analysis of this, Johnson et al. [8] show that at large momentum transfers break-up via neutron shakeoff must occur. This entails an important reduction of the elastic cross section at large scattering angles, not yet detected experimentally. As we shall show in the following, this same component has already been detected in the inelastic channel. Shakeoff is, generally speaking, characteristic of all processes in which momentum is imparted to the core. A prime example is Coulomb excitation, which cannot act directly on the halo neutron. The recent paper by Tostevin et al. [9] treats Coulomb break-up of the deuteron, the lightest halo system, in this spirit, and Pushkin et al. [10] give a convenient expression for the excitation energy spectrum from Coulomb excitation of ^{11}Li , which we shall make use of later. The same shakeoff distribution has been encountered in inelastic proton scattering on ^{11}Li [11].

In Sect. 2 we demonstrate how the shakeoff mechanism can be incorporated in the eikonal model for the break-up of halo nuclei developed in [1-3]. In Sect. 3 we apply the

theory to the break-up of ^{11}Be and ^{11}Li and compare with experimental data. Conclusions are collected in Sect. 4.

2 Break-up in the eikonal approximation

At intermediate and high incident energies, the reaction mechanism can be treated in the eikonal approximation, and it is appropriate to treat the development of the halo wavefunction in the sudden approximation [12]. The complete differential cross section for a two-body halo nucleus in the coordinate system of Fig. 1 is then given by (c.f.[6])

$$\frac{d\sigma}{d^2Qd^3q} = \frac{1}{(2\pi)^5} |A(\mathbf{Q}, \mathbf{q})|^2, \quad (1)$$

with

$$A(\mathbf{Q}, \mathbf{q}) = \int d^2b e^{-i\mathbf{Q}\cdot\mathbf{b}} \times \int d^3r \phi_{\mathbf{q}}^*(\mathbf{r}) (1 - S_1(\mathbf{b} + \beta_2 \mathbf{r}_t) S_2(\mathbf{b} - \beta_1 \mathbf{r}_t)) \phi_o(\mathbf{r}), \quad (2)$$

where ϕ_o is the ground state wavefunction, $\phi_{\mathbf{q}}$ is the two-body relative motion wavefunction with asymptotic relative momentum \mathbf{q} , \mathbf{Q} is the C.M. momentum, β_1 (β_2) is the ratio between the halo-neutron (core) mass and the mass of the halo nucleus, and S_1 and S_2 are the reaction profile functions of the neutron and the core respectively. Note that, because of the orthogonality between $\phi_{\mathbf{q}}$ and ϕ_o , it is equivalent to use $(1 - S_1 S_2)$ or just $S_1 S_2$, as we will do in the following.

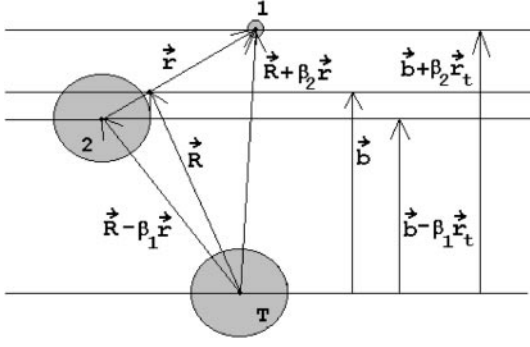


Fig. 1. Coordinate system used for describing the reaction mechanism: \mathbf{R} is the position vector of the halo nucleus C.M. with respect to the target, with \mathbf{b} its transverse component; \mathbf{r} is the relative position vector of the core and the neutron of the halo nucleus; $\mathbf{R} - \beta_1 \mathbf{r}$ is the position vector of the core with respect to the target, with $\mathbf{b} - \beta_1 \mathbf{r}_t$ its transverse component; $\mathbf{R} + \beta_2 \mathbf{r}$ is the position vector of the halo neutron with respect to the target, with $\mathbf{b} + \beta_2 \mathbf{r}_t$ its transverse component. Transverse components are referred to the direction of motion of the C.M. of the halo nucleus

By using the identities

$$S_1(\mathbf{b} + \beta_2 \mathbf{r}_t) = S_1(\mathbf{b} + \mathbf{r}_t) + [S_1(\mathbf{b} + \beta_2 \mathbf{r}_t) - S_1(\mathbf{b} + \mathbf{r}_t)] \quad (3)$$

$$S_2(\mathbf{b} - \beta_1 \mathbf{r}_t) = S_2(\mathbf{b}) + [S_2(\mathbf{b} - \beta_1 \mathbf{r}_t) - S_2(\mathbf{b})], \quad (4)$$

the amplitude (2) can be rewritten

$$A(\mathbf{Q}, \mathbf{q}) = A_{ND} + A_{SO} + A^* \quad (5)$$

where

$$A_{ND}(\mathbf{Q}, \mathbf{q}) = \int d^2 b e^{-i\mathbf{Q} \cdot \mathbf{b}} S_2(\mathbf{b}) \times \int d^3 r \phi_{\mathbf{q}}^*(\mathbf{r}) S_1(\mathbf{b} + \mathbf{r}_t) \phi_o(r), \quad (6)$$

$$A_{SO}(\mathbf{Q}, \mathbf{q}) = \int d^2 b e^{-i\mathbf{Q} \cdot \mathbf{b}} \times \int d^3 r \phi_{\mathbf{q}}^*(\mathbf{r}) S_1(\mathbf{b} + \mathbf{r}_t) \Delta S_2 \phi_o(r), \quad (7)$$

and

$$A^*(\mathbf{Q}, \mathbf{q}) = \int d^2 b e^{-i\mathbf{Q} \cdot \mathbf{b}} \times \int d^3 r \phi_{\mathbf{q}}^*(\mathbf{r}) (S_2(\mathbf{b}) \Delta S_1 + \Delta S_1 \Delta S_2) \phi_o(r), \quad (8)$$

with

$$\Delta S_1 = [S_1(\mathbf{b} + \beta_2 \mathbf{r}_t) - S_1(\mathbf{b} + \mathbf{r}_t)], \quad (9)$$

$$\Delta S_2 = [S_2(\mathbf{b} - \beta_1 \mathbf{r}_t) - S_2(\mathbf{b})]. \quad (10)$$

Integrating over \mathbf{Q} one obtains the relative momentum differential cross sections. For example,

$$\frac{d\sigma}{d^3 q} |_{ND} = \frac{1}{(2\pi)^3} \int d^2 b |S_2(\mathbf{b})|^2 |a(\mathbf{b}, \mathbf{q})|^2, \quad (11)$$

where

$$a(\mathbf{b}, \mathbf{q}) = \int d^3 r \phi_{\mathbf{q}}^*(\mathbf{r}) S_1(\mathbf{b} + \mathbf{r}_t) \phi_o(r). \quad (12)$$

The term A_{ND} describes the diffractive scattering of the halo neutron on the target. The neutron profile function acts on the internal ground state wavefunction ϕ_o . The modified wavefunction, $S_1 \phi_o$, will have an overlap with the excited states $\phi_{\mathbf{q}}$; if the latter are in the continuum, this leads to the break-up of the projectile. The factor $|S_2(\mathbf{b})|^2$ enters simply as a weighting factor; it gives the probability that the core survives after the collision for a given impact parameter \mathbf{b} .

For an infinitely heavy core, $\beta_1 = 0$ and $\beta_2 = 1 - \beta_1 = 1$ (as was assumed in [1-3]), the shakeoff amplitude, A_{SO} , vanishes since ΔS_2 goes to zero. This is the "no-recoil approximation" discussed by Bertsch et al. [7]. For small but not vanishing values of β_1 , the low \mathbf{q} part of A_{SO} is governed by the leading linear component of ΔS_2 , equation (10), which shows the relation between the center-of-mass motion and diffraction of the core. It turns out that the shakeoff term is significant for the applications to ^{11}Be and ^{11}Li and also that it is important to include the Coulomb contribution, for which we have $S_1 = 1$ and $A_{ND} = 0$. In practice the Coulomb contribution has been calculated using the Alder and Winther formalism [13], as is commonly done in the literature (cf. for example [14]).

We will neglect the contribution A^* ; we expect that it gives appreciable contributions only at high values of \mathbf{q} , since for small values of β_1 the leading term of $\Delta S_1 \simeq -\beta_1 \mathbf{r}_t \cdot \partial S_1 / \partial(\mathbf{b} + \mathbf{r}_t)$ is already a rapidly varying function of \mathbf{r}_t .

For simplicity, in evaluating A_{SO} we will also put the neutron reaction profile function S_1 equal to one, that is, we assume that the target is transparent to the neutron. Within this approximation ΔS_2 may be substituted by $S_2(\mathbf{b} - \beta_1 \mathbf{r}_t)$, since in virtue of the orthogonality between $\phi_{\mathbf{q}}$ and ϕ_o , $S_2(\mathbf{b})$ gives no contribution.

The shakeoff amplitude may be written in an very simple way by expressing the S_2 profile function in terms of its Fourier transform

$$\tilde{S}_2(\mathbf{K}) = \int d^2 s e^{-i\mathbf{K} \cdot \mathbf{s}} S_2(\mathbf{s}). \quad (13)$$

After integration over \mathbf{b} , one obtains

$$A_{SO}(\mathbf{Q}, \mathbf{q}) = \tilde{S}_2(\mathbf{Q}) \int d^3 r \phi_{\mathbf{q}}^*(\mathbf{r}) e^{-i\beta_1 \mathbf{Q} \cdot \mathbf{r}_t} \phi_o(r). \quad (14)$$

The neutron wavefunctions ϕ_o and $\phi_{\mathbf{q}}$ are taken to be the eigenfunctions of a zero range potential, as in previous studies. In [15] it has been shown that it is possible to make use of a simple finite size correction in order to reproduce the external wavefunctions of more realistic potentials, a correction that we neglect here in the spirit of a simple estimate. (It would improve the agreement with experiment, see Fig. 2). The expressions for ϕ_o and $\phi_{\mathbf{q}}$ are

$$\phi_o(r) = \sqrt{\frac{\eta}{2\pi}} \frac{e^{-\eta r}}{r} \quad (15)$$

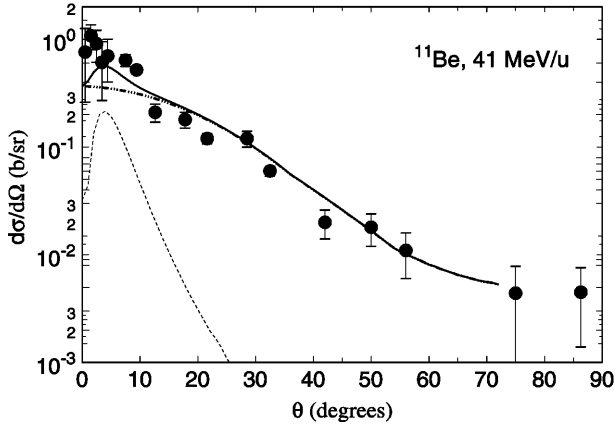


Fig. 2. Neutron angular distribution in the reaction $^{11}\text{Be} \rightarrow ^{10}\text{Be} + n$ at 41 MeV/n on a ^9Be target. The dashed-dotted line is the result for diffraction dissociation obtained in [5]. The dashed line is that obtained adding the shakeoff (nuclear and Coulomb) contributions, and the solid line is the sum of all contributions. The data points are from reference [15]. Note that the calculation presented does not include the finite-size correction [15], which would increase the shakeoff contribution by a factor of two and improve the agreement with experiment

$$\phi_{\mathbf{q}}(\mathbf{r}) = e^{i\mathbf{q}\cdot\mathbf{r}} + \frac{1}{iq - \eta} \frac{e^{-iqr}}{r} \quad (16)$$

The decay energy distribution arising from shakeoff may be obtained by integrating over \mathbf{Q} and the angular variables of \mathbf{q} . If the dipole approximation is used, the dipole energy distribution is found, that is

$$\frac{d\sigma}{dE}|_{SO} \propto \frac{E^{3/2}}{(E+B)^4}, \quad (17)$$

where E is the kinetic energy of the fragments in the C.M. frame, and B is the halo binding energy, related to the η parameter by the expression $B = \hbar^2\eta^2/2m$.

After integration over \mathbf{Q} and the longitudinal component of \mathbf{q} , the transverse momentum distribution may be calculated. In the dipole approximation the expression becomes

$$\frac{d\sigma}{dq_t}|_{SO} \propto \frac{q_t^3}{(\eta^2 + q_t^2)^{7/2}}, \quad (18)$$

which can be easily converted into angular distribution by using (for forward angles) $\theta_{LAB} \simeq q_t/k_o$, where k_o is the incident momentum per particle in the LAB system. The resulting expression is

$$\frac{d\sigma}{d\Omega}|_{SO} \propto \frac{\theta_{LAB}^2}{(\eta^2 + k_o^2\theta_{LAB}^2)^{7/2}}. \quad (19)$$

3 Comparison with experimental data

In this section we apply the formalism developed above to two different cases: $^{11}\text{Be} \rightarrow ^{10}\text{Be} + n$ at 41 MeV/n on a ^9Be target [15], and $^{11}\text{Li} \rightarrow ^9\text{Li} + 2n$ at 280 MeV/n on a ^{12}C target [16]. In the ^{10}Be case the angular distribution

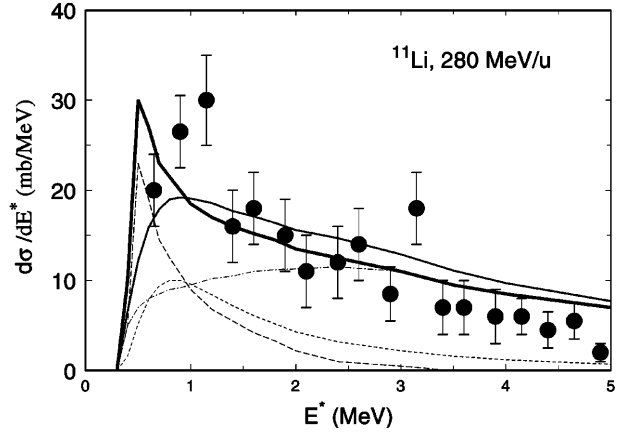


Fig. 3. Excitation energy (E^*) spectrum for the reaction $^{11}\text{Li} \rightarrow ^9\text{Li} + 2n$ at 280 MeV/n on a ^{12}C target. The data points are from reference [16]. The dashed-dotted line is the contribution of the halo-neutron diffraction. The strongly peaked distribution (long-dashed line) is the shakeoff contribution calculated according to our two-body model. The thick solid line is that obtained adding the shakeoff and the diffraction contributions. The broad distribution (short-dashed line) represents the dipole shape calculated in a three-body model by Pushkin et al. [10] scaled to our calculated shakeoff integrated cross section. The thin solid line is that obtained summing the latter with the diffraction contribution

of neutrons is analyzed, while in the ^{11}Li we calculate the decay energy. In both cases the distribution arising from the shakeoff mechanism is added to that corresponding to the neutron-diffraction. The latter has been calculated, for example, in references [2, 3, 5, 15]. Where required, the momentum distributions were translated into energy distribution by means of a Jacobian transformation. In what follows the black-disc model for the nuclear profile functions is used, with a 1fm^{-1} cut-off in the momentum space, which is roughly equivalent to a 1fm diffusivity in normal space.

In Fig. 2 the angular distribution of the neutrons arising from the ^{10}Be break-up is presented. The contribution from neutron diffraction has been taken from the realistic calculation of [5], which compares quite well with that of the black-disc calculation of [15]. The integrated cross section is about 260 mb. It must be noted that interference between A_{ND} and A_{SO} has been neglected, what we believe is reasonable given their very different dependence on angle and momentum.

The integrated shakeoff cross section is 16 mb, of which 7 mb are from nuclear shakeoff and 9 mb are from Coulomb break-up. Despite the much smaller integrated cross section, the contribution from shakeoff is clearly visible at small angles. The experimental data clearly point to the existence of such effects, although the error bars are quite large [15].

In Fig. 3 we show the excitation energy ($E^* = E + B$) distribution of the ^{11}Li break-up. The main contribution arises from diffraction dissociation of a halo neutron followed by the sequential decay of ^{10}Li , as discussed in [1-3].

This cross section has been scaled in order to reproduce the high energy tail of the distribution. To this is added the distribution produced by shakeoff, which gives rise to a peak at low energies. This cross section is multiplied by a factor of two due to the presence of two neutrons in the ^{11}Li halo. From this procedure it turns out that the integrated cross section associated to neutron-diffraction and to shakeoff are now much closer, namely, 57 mb and 23 mb (15 mb of nuclear type and 8 mb from Coulomb break-up) respectively.

Thus, this analysis reveals a different energy dependence for neutron diffraction and shakeoff. The explanation for this may be found in the increased transparency of the target for the halo neutron as the bombarding energy increases, while for the core, a much more complex object, the opacity assumed in the black-disc model should still be valid at higher energies. A detailed calculation in terms of nucleon-nucleon cross section and its energy dependence (c.f. [6]) is left for further studies.

The energy of the peak in Fig. 3 is lower than the experimental one. In this sense it must be noted that in the calculations we have used the dipole energy distribution of equation (17), which is appropriate for a two-body system. It is known that for a three-body system, as ^{11}Li , a shift to higher energies is expected. We show for comparison in Fig. 3 the contribution based on the analytical expression given by Pushkin et al. [10], which leads to a shape of the excitation energy spectrum in better agreement with the data, but that underestimates the height of the low energy peak. In this respect it should be noted that the correlations between the halo-neutrons neglected in our calculations tend to increase the dipole strength at low energy [17]. It is interesting to observe that, from our model, for heavier targets, as lead for example, where the Coulomb break-up is the dominant mechanism, a similar peak is expected, since also in this case the dipole component is the dominant one. This is indeed what is experimentally observed [16].

4 Conclusions

We conclude that including the shakeoff mechanism gives a significantly better understanding of the experimental data. In particular, it leads to a sizeable increase in the differential cross sections at small angles, which is observed

experimentally in ^{11}Be break-up on a beryllium target, and was not previously explained. Shakeoff also produces a peak at low energy in the ^{11}Li decay energy spectrum after break-up on a carbon target, again in qualitative agreement with experiment.

Discussions with Enrico Vigezzi are gratefully acknowledged.

This work was supported by the U.S. National Science Foundation, grant number PHY-9528844.

References

1. F. Barranco and E. Vigezzi, in Proc. of the 4th Course of the International School of Heavy-Ion Physics (Eds. R.A. Broglia and P.G. Hansen, World Scientific, Singapore) pp. 217-254
2. F. Barranco, E. Vigezzi and R.A. Broglia, Phys. Lett. B319, 387 (1993)
3. F. Barranco, E. Vigezzi and R.A. Broglia, Z. Phys. A356, 45 (1996)
4. P.G. Hansen, Phys. Rev. Lett. 77, 1016 (1996)
5. A. Bonaccorso and D. Brink, Phys. Rev. C57 (1998), R22 (1998)
6. K. Hencken, G. Bertsch and H. Esbensen, Phys. Rev. C54, 3043 (1996)
7. G.F. Bertsch, K. Hencken and H. Esbensen, Phys. Rev. C57, 1366 (1998)
8. R.C. Johnson, J.S. Al-Khalili and J.A. Tostevin, Phys. Rev. Lett. 79, 2771 (1997)
9. J.A. Tostevin, S. Rugmai and R.C. Johnson, Phys. Rev. C57, 3225 (1998)
10. A. Pushkin, B. Jonson and M.V. Zhukov, J. Phys. G: Nucl. Part. 22, L-95 (1996)
11. S. Karataglidis, P.G. Hansen, B.A. Brown, K. Amos and P.J. Dortmans, Phys. Rev. Lett. 79, 1447 (1997)
12. L. Landau and E. Lifshitz, Quantum Mechanics (3th ed.), pg. 152
13. A. Winther and K. Alder, Nucl. Phys. A319, 518 (1979)
14. H. Esbensen, in Proc. of the 4th Course of the International School of Heavy-Ion Physics (Eds. R.A. Broglia and P.G. Hansen, World Scientific, Singapore) pp. 71-92
15. R. Anne et al., Nucl. Phys. A575, 125 (1994)
16. M. Zinser et al., Nucl. Phys. A619, 151 (1997)
17. H. Esbensen and G.F. Bertsch, Nucl. Phys. A542, 310 (1992)